# Determination of Depositional Beryllium-10 Fluxes in the Area of the Laptev Sea and Beryllium-10 Concentrations in Water Samples of High Northern Latitudes

**C. Strobl[1], V. Schulz[1], S. Vogler[1], S. Baumann[1], H. Kassens[2], P.W. Kubik[3], M. Suter[4] and A.Mangini[1]**

*(1) Heidelberger Akademie der Wissenschaften, Im Neuenheimer Feld 366, D 69120 Heidelberg, Germany*

*(2) GEOMAR Forschungszentrum für marine Geowissenschaften, Wischhofstrasse 1-3, D 24148 Kiel, Germany*

*(3) Paul Scherrer Institut, c/o Institut für Partikelphysik, ETH Hönggerberg, 8093 Zürich, Switzerland*

*(4) Institut für Partikelphysik, ETH Hönggerberg, 8093 Zürich, Switzerland*

Received 20 February 1997 and accepted in revised form 9 May 1998

**Abstract** - Present day accumulation rates of nine sediment cores recovered during the Russian-German Expedition Transdrift II (1994) from the shelf area of the Laptev Sea were determined by $^{210}Pb_{ex}$ dating and vary from 0.05 to 0.24 g $cm^{-2}$ $a^{-1}$. In addition, the sedimentation rates during the isotopic stages 2, 3 and 5 of the sediment core PS 2471-4 from the continental slope of the Laptev Sea were determined via $^{230}Th_{ex}$ dating. The $^{10}Be$ concentrations together with the accumulation rates (or sedimentation rates) yield the depositional $^{10}Be$ fluxes in the shelf area of [(10 - 150) $\cdot 10^6$ at $cm^{-2}$ $a^{-1}$] and of [(0.9 - 4.1) $\cdot 10^6$ at $cm^{-2}$ $a^{-1}$] on the continental slope from the Laptev Sea. They are clearly higher than the recent atmospheric input determined in Greenland ice cores [(0.2 - 0.5) $\cdot 10^6$ at $cm^{-2}$ $a^{-1}$]. We conclude that large amounts of continental $^{10}Be$ are delivered to the Laptev Sea through the rivers (e.g. Lena,Yana) and that the major fraction of $^{10}Be$ is deposited directly in the shelf area. The distinctly higher concentrations of $^{10}Be$ in water samples from the shelf area of the Laptev Sea [1000 to 6000 at/g] compared to the concentrations measured in the Norwegian and Greenland Sea [300 to 1000 at/g] and the Central Arctic Ocean [500 at/g] are further evidence that rivers are an important source for the input of $^{10}Be$ from the Siberian hinterland to the Arctic Ocean.

## Introduction

The cosmogenic radionuclide $^{10}Be$ ($t_{1/2}$ = 1.5 Ma) is a sensitive stratigraphic tool for sediments from the Arctic Ocean with low or negligible content of biogenic carbonate. $^{10}Be$ records from sediment cores from the Norwegian and Greenland Sea exhibit high concentrations of $^{10}Be$ during the interglacials in contrast to lower values during glacial periods (Eisenhauer et al., 1994). These distinct changes enable a glacial/interglacial stratigraphy of Arctic sediments. Better knowledge of the pathways of $^{10}Be$ from the Laptev Shelf into the sediments of the Arctic Ocean could render the records from sediment cores of the Arctic Ocean more reliable. As part of the Russian-German cooperative research project "System Laptev Sea" we focussed on the evaluation of supply and export fluxes of $^{10}Be$ in the shelf area and on the continental slope of the Laptev Sea. The atmospheric input was measured in ice cores from the Greenland Ice Sheet (Stanzick, 1996). The supply of $^{10}Be$ with the river was determined from the measurement of water samples from the estuary of the river Lena. For comparison we also measured profiles of the $^{10}Be$ contentration at three localities in the central Arctic Ocean. The amount of riverine $^{10}Be$ deposited on the shelf was evaluated from the concentration of $^{10}Be$ in shelf sediments. The accumulation rates of the sediments were determined from profiles of $^{210}Pb_{ex}$.

In: Kassens, H., H.A. Bauch, I. Dmitrenko, H. Eicken, H.-W. Hubberten, M. Melles, J. Thiede and L. Timokhov (eds.) Land-Ocean Systems in the Siberian Arctic: Dynamics and History. Springer-Verlag, Berlin, 1999, 515-532.

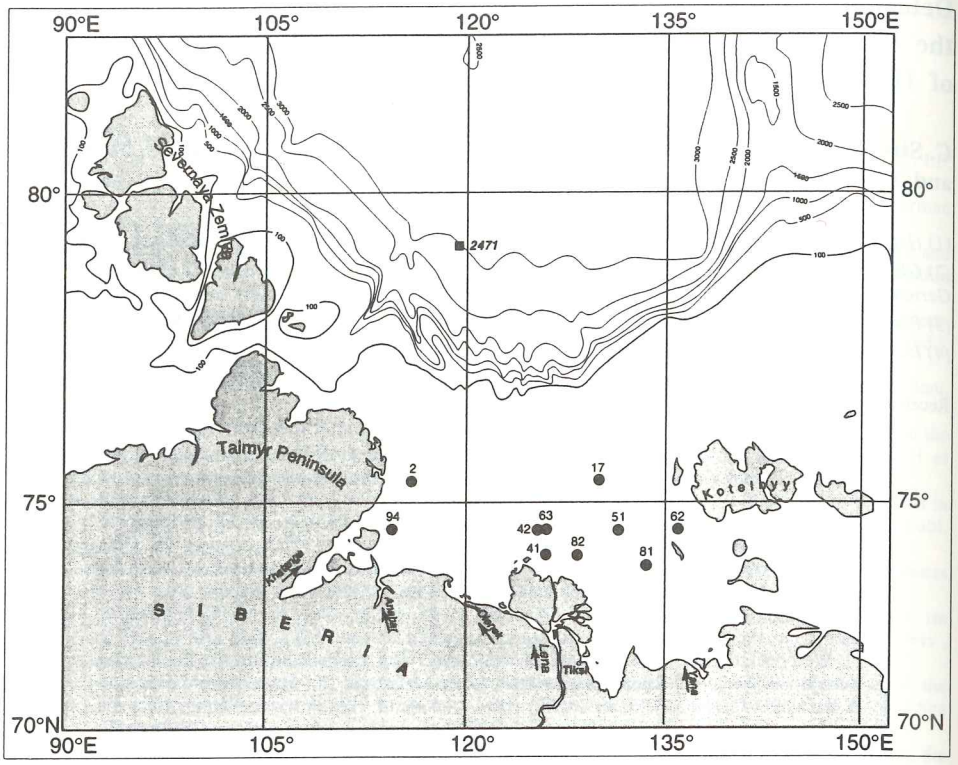


Figure 1: Map showing the locations of the investigated sediment cores and water profiles in the Laptev Sea.

Table 1: Locations of the sediment cores from the shelf area and from the continental slope

| Station | Location | Water Depth [m] | Core Length [cm] |
|---|---|---|---|
| PM 9402-3 (GKG) | 75°29.44`N, 115°14.94`E | 47 | 39 |
| PM 9417-4 (GKG) | 75°30.17`N, 130°00.83`E | 51 | 45 |
| PM 9441-4 (GKG) | 74°00.01`N, 125°59.35`E | 14 | 19 |
| PM 9442-3 (GKG) | 74°30.05`N, 126°00.20`E | 40 | 47 |
| PM 9451-7 (GKG) | 74°30.16`N, 130°29.70`E | 25 | 18 |
| PM 9462-1 (GKG) | 74°30.13`N, 136°00.23`E | 27 | 53 |
| PM 9462-4 (VC) | 74°30.18`N, 136°00.32`E | 27 | 467 |
| PM 9463-8 (GKG) | 74°30.21`N, 126°34.91`E | 36 | 44 |
| PM 9481-2 (GKG) | 73°45.00`N, 134°00.25`E | 17 | 35 |
| PM 9482-1 (GKG) | 73°59.94`N, 128°10.47`E | 27 | 56 |
| PS 2471-4 (KAL) | 79°09.07`N, 119°47.55`E | 3047 | 417 |

## Material and methods

The sediment cores (Table 1) investigated in our study were recovered during the Expeditions Transdrift II (Kassens,1995) and ARK IX/4 (Fütterer, 1994). Further we determined the $^{10}Be$ concentrations of 4 water profiles from the Norwegian and Greenland Sea (Thiede and Hempel, 1991), 3 profiles from the central Arctic Ocean (Fütterer, 1992) and water samples from the shelf area of the Laptev Sea (Kassens,1995). Their locations are listed in Table 2. All locations are plotted in Figures 1 and 2.

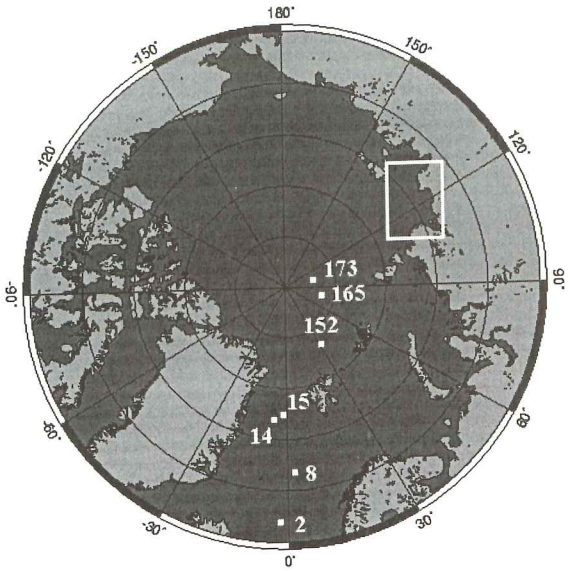


Figure 2: Map showing the locations of the investigated water profiles in the Norwegian- and Greenland Sea and the Central Arctic Ocean.

*Preparation and measurement of sediment samples*

The activities of the radionuclides $^{214}Bi$, $^{210}Pb$ and of the anthropogenic $^{137}Cs$ were measured by γ-spectroscopy. For the γ-spectroscopy the dried samples (10- 30 g) were filled into 50 ml polyethylene vials and counted on two low-level HPGe detectors. The detector efficiency was calibrated applying standards of known activity but differing geometries and densities prepared from a multi-nuclide standard (QCY44, Amersham). The radioisotopes $^{230}Th$, $^{232}Th$, $^{234}U$, $^{238}U$ were measured by α-spectroscopy. The sample material (0.5 g) was dried and homogenized. The chemical separation of these isotopes followed the procedure of Mangini (1984) and is described by Frank et al. (1994). The concentration of the radioisotope $^{10}Be$ was measured via accelerator mass spectrometry (AMS) at the tandem facility of the ETH Zürich and calibrated to an internal standard (S555) with a $^{10}Be/^{9}Be$ ratio of $95.5 \cdot 10^{-12}$. The chemical preparation of $^{10}Be$ followed the method described by Henken-Mellies et al. (1990) with minor modifications.

*Preparation of water samples*

Water samples from the Norwegian- and Greenland Sea, the central Arctic Ocean and the Laptev Sea of about 30 l were acidified with HCl to pH ≅ 2 and spiked with the stable $^{9}Be$-Isotope (1 ml). The chemical preparation followed the method described by Segl et al. (1987).

Table 2: Locations of the water profiles where $^{10}Be$ measurements have been performed.

| Sample | Location | Water Depth [m] | Sampled Depths [m] |
|---|---|---|---|
| Norwegian- and Greenland Sea | | | |
| 2 | 69°47`N, 15°39`W | 1189 | 6, 50, 250, 750 |
| 8 | 70° 45`N, 05°25`W | 2387 | 6, 100, 200, 500, 1000, 1500, 1950 |
| 14 | 75°25`N, 07°20`W | 3360 | 6, 50, 100, 200, 500, 1000, 1500, 2000 |
| 15 | 75°50`N, 08°10`W | 1970 | 6, 50, 100, 200, 500, 1000, 1500 |
| Central Arctic Ocean | | | |
| 152 | 83°58.5`N, 30°24.8`E | 3890 | 50, 500, 1500, 2250, 3000, 3500 |
| 165 | 87°34.4`N, 60°23.1`E | 4300 | 50, 500, 1300, 2300, 3300, 4300 |
| 173 | 87°45.2`N, 108°59.1`E | 4220 | 50, 320, 1220, 2220, 3220, 4220 |
| Laptev Sea | | | |
| PM 9463-1 | 74°30.07`N, 126°35.06`E | 36 | 2, 30 |
| PM 9472-3 | 71°59.85`N, 130° 30.77`E | 16 | 2 |
| PM 9494-3 | 74°30.06`N, 114°17.05`E | 36 | 2 |

## Results

*Determination of the Accumulation Rates in the Shelf Area of the Laptev Sea*

$^{210}Pb$

The Constant-Flux $^{210}Pb_{ex}$ method has been often applied for dating sediment cores from lakes and estuaries (Dominik et al., 1981; Doerr et al., 1991; von Gunten et al., 1993; Bollhoefer et al., 1994). It relies on the assumption that the atmospheric $^{210}Pb$ deposition remained constant over the last century. This atmospheric component of $^{210}Pb$ ($^{210}Pb_{ex}$), decays in the sediment column with a half life of 22.3 years. It can be determined from the measured $^{210}Pb$ ($^{210}Pb_{tot}$) specific activity minus a component which is produced by the in situ-decay of $^{226}Ra$ in detritic material ($^{210}Pb_{supp}$) and another component produced by the decay of dissolved $^{226}Ra$ in the water column. Because of the low water depth of 50 m in the shelf area of the Laptev Sea this last component can be neglected. Thus the $^{210}Pb_{ex}$ activity of each sample was determined as:

$$^{210}Pb_{ex} = {}^{210}Pb_{tot} - {}^{210}Pb_{supp} \qquad (1)$$

The activity of the supported $^{210}Pb$ corresponds to the specific activity of the $^{214}Bi$ ($t_{1/2}$ = 20 min) which is assumed to be in radioactive equilibrium with its mother $^{226}Ra$. Therefore the $^{210}Pb_{ex}$ activity can be calculated as:

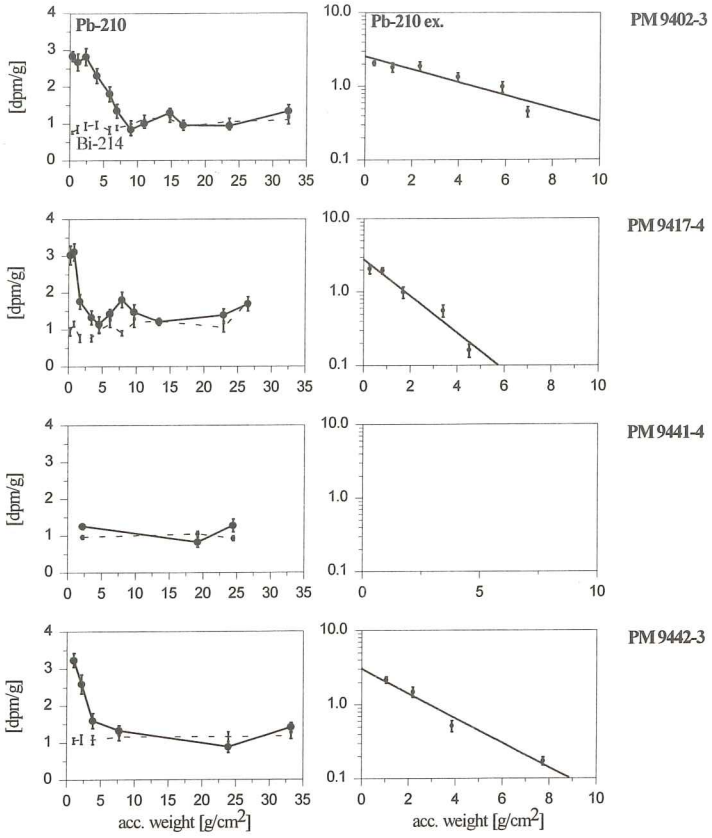


Figure 3: Activities of $^{210}Pb_{tot}$, $^{210}Pb_{ex}$ and $^{214}Bi$ plotted against compaction-corrected depth. On the plots on the right the $^{210}Pb_{ex}$ activities are presented on a logarithmical scale.

$$^{210}Pb_{ex} = {}^{210}Pb_{tot} - {}^{214}Bi \qquad (2)$$

The activities of $^{210}Pb_{tot}$, $^{210}P_{ex}$, and $^{214}Bi$ are plotted against compaction-corrected depth in Figures 3 and 4. The right diagrams show the profiles of the $^{210}Pb_{ex}$ activities on a logarithmical scale. The mean accumulation rate (R) and sedimentation rate (S) can be calculated from the slope of the best exponential fit to $^{210}P_{ex}$ as:

$$^{210}Pb_{ex}(G) = {}^{210}Pb_{ex}(0) \cdot e^{-\lambda \cdot G/R} \qquad (3)$$

$$R = \lambda \cdot G \cdot (\ln ({}^{210}Pb_{ex}(G)/{}^{210}Pb_{ex}(0)))^{-1} \qquad (4)$$

$$S = R / \rho \qquad (5)$$

where:
G : compaction corrected depth [g $cm^{-2}$]
$^{210}Pb_{ex}(0)$ : $^{210}Pb_{ex}$ activity at the surface

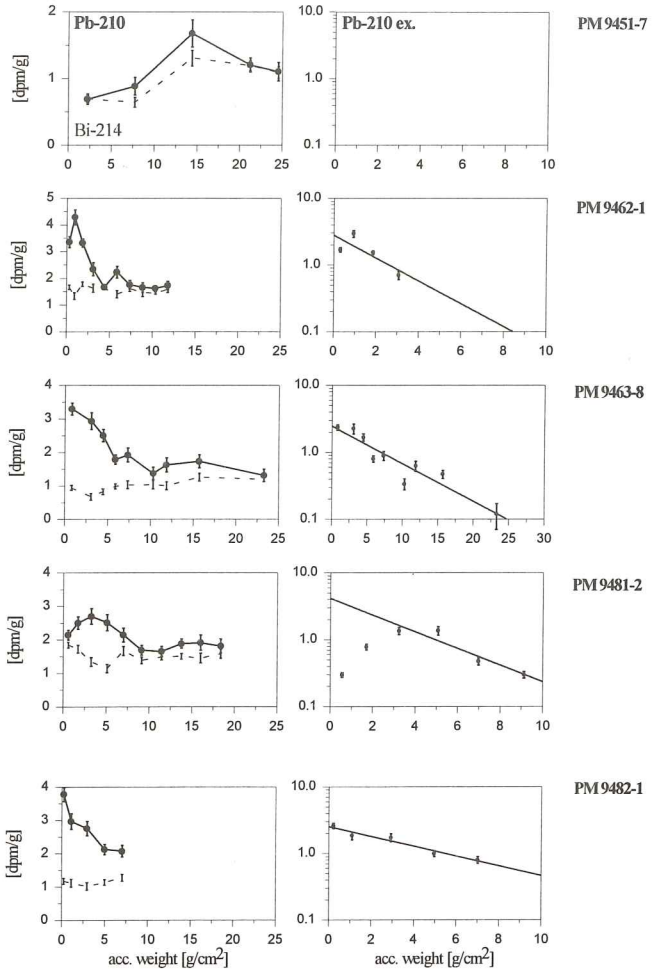


Figure 4: Activities of $^{210}Pb_{tot}$, $^{210}Pb_{ex}$ and $^{214}Bi$ are plotted against compaction-corrected depth. On the plots on the right the $^{210}Pb_{ex}$ activities are presented on a logarithmical scale.

$\lambda$ : decay constant of $^{210}Pb$ [0.031 $a^{-1}$]
$\rho$ : dry bulk density [g $cm^{-3}$]
R : mean accumulation rate [g $cm^{-2}a^{-1}$]
S : mean sedimentation rate [cm $a^{-1}$]

The mean accumulation rates [g $cm^{-2}$ $a^{-1}$] , the average dry bulk densities (pers. comm. Kassens, 1995), and the sedimentation rates [cm $a^{-1}$] of the investigated cores are listed in Table 3. The sediment cores PM 9441-4 and PM 9451-7 could not be dated because we did not find any $^{210}Pb_{ex}$ at all. This lack of $^{210}Pb_{ex}$ could be ascribed either to dilution with sediments accumulating at a very high rate or to conditions preventing accumulation of recent sediment. The sandy composition of these sediments suggests possible export of the fine grain fraction. However, bioturbative mixing of $^{210}Pb$ at the sediment water interface may distort the profiles

of the radionuclides and lead to apparent larger accumulation rates (Berner, 1980; Benninger et al., 1980; Mangini et al., 1986). The apparent contribution due to mixing can be evaluated as an additional accumulation rate ($S_{diff}$) (Mangini et al., 1988) given as:

$$S_{diff} = D \cdot \lambda / S \qquad (6)$$

where S is the accumulation rate derived from the depth profile of the radioisotope and D is the effective diffusion coefficient.

Table 3: Average bulk densities, accumulation and sedimentation rates of the investigated sediment cores from the shelf area of the Laptev Sea.

| Station | Accumulation rate (R) | Bulk density | Sedimentation rate (S) |
|---|---|---|---|
| | [g $cm^{-2}$ $a^{-1}$] | [g $cm^{-3}$] | [cm $a^{-1}$] |
| PM 9402-3 | 0.15 ± 0.03 | 0.95 | 0.16 ± 0.03 |
| PM 9417-4 | 0.05 ± 0.02 | 0.73 | 0.08 ± 0.03 |
| PM 9441-4 | no dating | | |
| PM 9442-3 | 0.08 ± 0.01 | 0.62 | 0.13 ± 0.02 |
| PM 9451-7 | no dating | 1.62 | |
| PM 9462-1 | 0.08 ± 0.02 | 0.69 | 0.12 ± 0.03 |
| PM 9463-8 | 0.24 ± 0.04 | 0.69 | 0.35 ± 0.06 |
| PM 9481-2 | 0.19 ± 0.08 | 1.15 | 0.17 ± 0.07 |
| PM 9482-1 | 0.19 ± 0.01 | 0.49 | 0.39 ± 0.02 |

Mixing coefficients below the topmost layers of Long Island Sound sediments, are in the range of 0.6 $cm^2$ $a^{-1}$ (Benninger et al., 1980), and are significantly lower in pelagic sediments from the Norwegian Sea (range 0.02 — 0.5 $cm^2$ $a^{-1}$, Arnold, 1989).

Obviously, the smallest distortion will be in those cores where the profile of $^{210}Pb_{ex}$ can be detected to the deepest depths into the sediments and where the apparent accumulation rates derived from the depth distribution are highest. In the two cores, PM9463-8 and PM9482-1, where excess $^{210}Pb$ is detected up to about 30 to 40 cm depth, distortion due to bioturbative mixing should be smallest.

Applying a value of 0.6 $cm^2$ $a^{-1}$ and an accumulation rate of 0.4 cm $a^{-1}$, the apparent contribution to accumulation rate can be evaluated at 0.05 cm $a^{-1}$. Thus the distortion due to mixing in these two cores lies within the uncertainty of the accumulation rate.

### $^{137}Cs$

The artificial radionuclide $^{137}Cs$ delivers an independent time mark to test our datings with $^{210}Pb_{ex}$. The first appearance of this isotope in sediments corresponds to the beginning of the

nuclear tests in 1954. The maximum fall-out corresponds to 1963. The function of atmospheric input of $^{137}Cs$ is plotted in Figure 5. The $^{137}Cs$ records of the investigated sediment cores are plotted against $^{210}Pb_{ex}$ ages (Figure 6) calculated from the mean sedimentation rates listed in Table 3. The top of the sediment cores was fixed to 1994. The two cores displaying the fastest accumulation rates, from localities PM 9463-8 and PM 9482-1, show very good agreement between the $^{210}Pb_{ex}$ timescale and the first appearance of $^{137}Cs$. In the other 6 cores the agreement is rather good. However, in these cores we detected $^{137}Cs$ activities in layers older than 1940 (dated with $^{210}Pb_{ex}$), which are in evident discrepancy to the timescale of bomb $^{137}Cs$ (Figure 5). This discrepancy originates either from a wrong (to small) evaluation of the accumulation rate with $^{210}Pb_{ex}$, or from postdepositional migration of $^{137}Cs$ in the sediments. The latter was suggested to happen in anoxic sediments (Evans et al. 1983). As the sediments from the shelf area become suboxic within few cm depth below the surface (Langner et al., 1995), we cannot exclude some migration of $^{137}Cs$ to have occurred. Because of the larger uncertainty of the accumulation rates from $^{210}Pb_{ex}$ in these cores we cannot address this question properly.

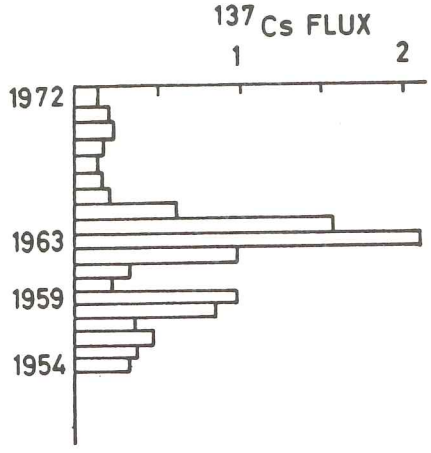


Figure 5: Atmospheric flux of $^{137}Cs$ in relative units (after Robbins and Edgington, 1976).

Standing Crop of $^{210}Pb_{ex}$

Comparison of the Standing crop of $^{210}Pb_{ex}$ in cores with uncertain accumulation rates with the one of core PM 9463-8 allows an additional test of their average accumulation rates. The Standing crop (SC) of $^{210}Pb_{ex}$ is defined as:

$$SC = \int_0^\infty \rho(x)A(x)dx \qquad (7)$$

where:

x : core depth [cm]

ρ : dry bulk density [g $cm^{-3}$]

A : $^{210}Pb_{ex}$ activity [dpm $g^{-1}$]

In the other cores, where $^{210}Pb$ does not penetrate as deep, we are aware that mixing may significantly distort the depth profiles of $^{210}Pb_{ex}$. In these other cores we evaluate the accumulation rate by comparison of their SC with the one of core PM9463-8 under the

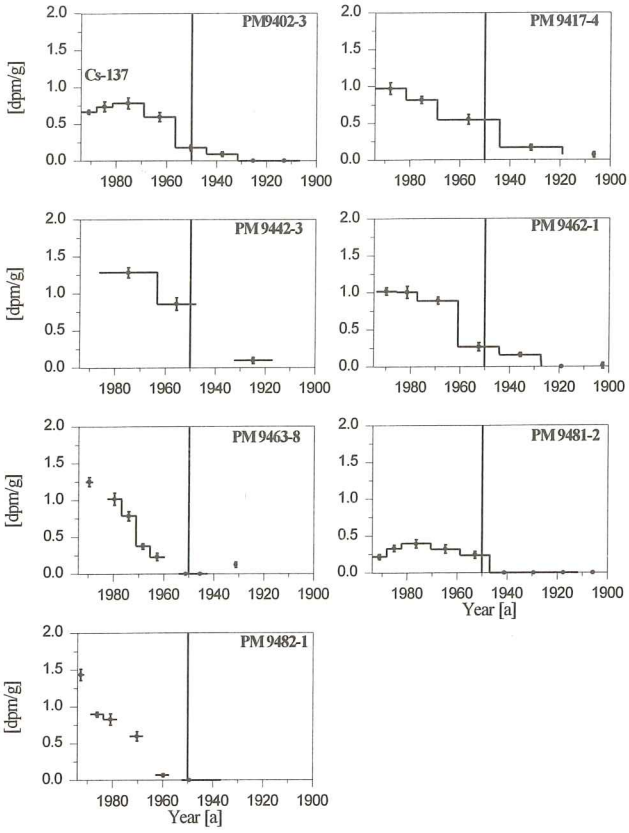


Figure 6: $^{137}Cs$ records of the investigated sediment cores against $^{210}Pb$ ages. The line represent the time mark 1950.

assumption that the flux density $^{210}Pb$ into the sediments and the concentration of sedimenting material has remained constant. A smaller SC then the SC of the sediment core PM9463-8 corresponds to a smaller accumulation due to sediment winnowing, a larger Sc to sediment focussing.

$$R_x = \frac{R_{63}}{Sc_{63}} \cdot Sc_x \qquad (8)$$

$R_{63}$: mean accumulation rate of core PM 9463-8 [g cm$^{-2}$a$^{-1}$]
$R_x$: mean accumulation rate of core x [g cm$^{-2}$ a$^{-1}$]
$SC_{63}$: Standing Crop of core PM 9463-8 [dpm cm$^{-2}$]
$SC_x$: Standing Crop of core x [dpm cm$^{-2}$]

As listed in Table 4 the rates derived with this equation are similar to the ones derived from the depth profiles of $^{210}Pb_{ex}$. The deviations range within the uncertainties, suggesting that the rates derived from the $^{210}Pb_{ex}$ profiles are not significantly distorted by bioturbative mixing of

the sediment even at those localities with lower accumulation rates. Further the comparison of the average accumulation rates with the $^{210}Pb_{ex}$ method of 0.12 ± 0.02 cm $a^{-1}$ (PM9462-1) is in the same range as the accumulation rate derived by $^{14}C$ dating of 0.06 ± 0.02 cm a-1 (PM9462-4) (Bauch, pers. comm.) therefore the bioturbative processes can be only of small influence.

Table 4: Accumulation rates derived from the depth profiles of $^{210}Pb_{ex}$ and the Standing crop method

| Station | Accumulation Rate $^{210}Pb_{ex}$ [g $cm^{-2}$ $a^{-1}$] | Accumulation Rate Standing Crop [g $cm^{-2}$ $a^{-1}$] |
|---|---|---|
| PM9402-3 | 0.15 ± 0.03 | 0.14 ± 0.04 |
| PM9417-4 | 0.05 ± 0.02 | 0.09 ± 0.03 |
| PM9442-3 | 0.08 ± 0.01 | 0.10 ± 0.04 |
| PM9462-1 | 0.08 ± 0.02 | 0.13 ± 0.04 |
| PM9481-2 | 0.19 ± 0.08 | 0.11 ± 0.04 |

Table 5: Depositional $^{210}Pb_{ex}$ fluxes of sediment cores from the shelf area of the Laptev Sea.

| Station | Depositional $^{210}Pb_{ex}$ Fluxes [dpm $cm^{-2}$ $a^{-1}$] |
|---|---|
| PM 9402-3 | 0.35 ± 0.02 |
| PM 9417-4 | 0.22 ± 0.02 |
| PM 9442-3 | 0.25 ± 0.04 |
| PM 9462-1 | 0.31 ± 0.02 |
| PM 9463-8 | 0.60 ± 0.05 |
| PM 9481-2 | 0.26 ± 0.02 |

Depositional $^{210}Pb_{ex}$ fluxes in the shelf area of the Laptev Sea

At steady state, the Standing crop of excess $^{210}Pb$ must be balanced by the net flux of $^{210}Pb_{ex}$ into the sediment. The depositional $^{210}Pb_{ex}$ flux can be determined as:

$$F = \lambda \cdot SC \qquad (9)$$

F : depositional $^{210}Pb$ flux [dpm $cm^{-2}$ $a^{-1}$]
SC : Standing Crop [dpm $cm^{-2}$]
$\lambda$ : decay constant of $^{210}Pb$ [0.031 $a^{-1}$]

The depositional $^{210}Pb_{ex}$ fluxes of the investigated locations are listed in Table 5. The atmospheric supply of $^{210}Pb$ in different regions of the world ranges between 0.15 and 1.5 dpm $cm^{-2}$ $a^{-1}$ (Graustein and Turekian, 1986; Gopalakrishnan et al., 1973; Turekian et al.,

1977). Our data suggest an atmospheric flux of $^{210}Pb$ for the area of the Laptev Sea ≤ 0,6 dpm $cm^{-2}$ $a^{-1}$, which is in agreement with model results of Rehfeld (1994).

*Sedimentary $^{10}Be$-Fluxes in the Shelf Area of the Laptev Sea*

The sedimentation rates from Table 3 were used to calculate the depositional $^{10}Be$ flux into the sediments of the shelf area from the Laptev Sea. The depositional $^{10}Be$ flux is defined as:

$$F(x) = C(x) \cdot S(x) \cdot \rho(x) \qquad (10)$$

where:
F : depositional $^{10}Be$ flux [at $cm^{-2}$ $a^{-1}$]
C : concentration of $^{10}Be$ [atoms $g^{-1}$]
S : sedimentation rate [cm $ka^{-1}$]
ρ : dry bulk density [g $cm^{-3}$]

In Table 6 the $^{10}Be$ concentrations and the depositional $^{10}Be$ fluxes of the investigated sediment cores are listed. These $^{10}Be$ fluxes of [(10 - 150) $\cdot 10^6$at $cm^{-2}$ $a^{-1}$] in the shelf area of the Laptev Sea, are by two orders of magnitude higher than the recent atmospheric input [(0.2 - 0.5) $\cdot 10^6$ at $cm^{-2}$ $a^{-1}$ ] in Greenland (Stanzick, 1996) and other world regions (Table 7). This surplus of $^{10}Be$ indicates a significant supply of continental $^{10}Be$ with the rivers into the Laptev Sea during the last century.

Table 6: Measured $^{10}Be$ concentrations and the calculated $^{10}Be$ depositional fluxes.

| Station | Depth [cm] | $^{10}Be$ [$10^8$ atoms $g^{-1}$] | Depositional $^{10}Be$ Flux [$10^6$ atoms $cm^{-2}$ $a^{-1}$] |
|---|---|---|---|
| PM 9402-3 | 0 - 1 | 2.95 ± 0.23 | 36.8 ± 8.0 |
| PM 9402-3 | 14 - 16 | 3.28 ± 0.16 | 48.8 ± 10.0 |
| PM 9402-3 | 32 - 36 | 3.53 ± 0.14 | 49.1 ± 10.0 |
| PM 9417-4 | 0 - 1 | 4.62 ± 0.32 | 19.9 ± 3.0 |
| PM 9451-7 | 1 - 2 | 0.56 ± 0.11 | |
| PM 9462-1 | 0 - 1 | 3.53 ± 0.16 | 26.0 ± 3.0 |
| PM 9462-1 | 14 - 16 | 4.49 ± 0.21 | 40.5 ± 5.0 |
| PM 9463-8 | 1 - 2 | 3.93 ± 0.30 | 72,9 ± 15,0 |
| PM 9463-8 | 14 - 16 | 4.02 ± 0.31 | 105.6 ± 21.0 |
| PM 9463-8 | 32 - 36 | 4.78 ± 0.23 | 105.4 ± 21.0 |
| PM 9481-2 | 1 - 2 | 1.87 ± 0.19 | 36.2 ± 8.0 |
| PM 9481-2 | 14 - 16 | 1.99 ± 0.10 | 38.9 ± 7.0 |
| PM 9482-1 | 0 - 1 | 4.10 ± 0.44 | 68.6 ± 12.0 |

Table 7: Atmospheric $^{10}$Be fluxes as determined at other locations.

| Atmospheric $^{10}$Be fluxes | References | Investigated material |
|---|---|---|
| 1.21 ± 0,26 $\Sigma 10^6$ at cm$^{-2}$ a$^{-1}$ | Monaghan, 1985/86 | North America, Precipitation |
| 1.50 ± 0.50 $\Sigma 10^6$ at cm$^{-2}$ a$^{-1}$ | Lao et al., 1992 a/b | Pacific, Sediments |
| ~ 0.7 $\Sigma 10^6$ at cm$^{-2}$ a$^{-1}$ | Southon et al., 1987 | North Atlantic, Sediments |
| ~ 0.3 $\Sigma 10^6$ at cm$^{-2}$ a$^{-1}$ | Finkel et al., 1977 | Arctic, Sediments |

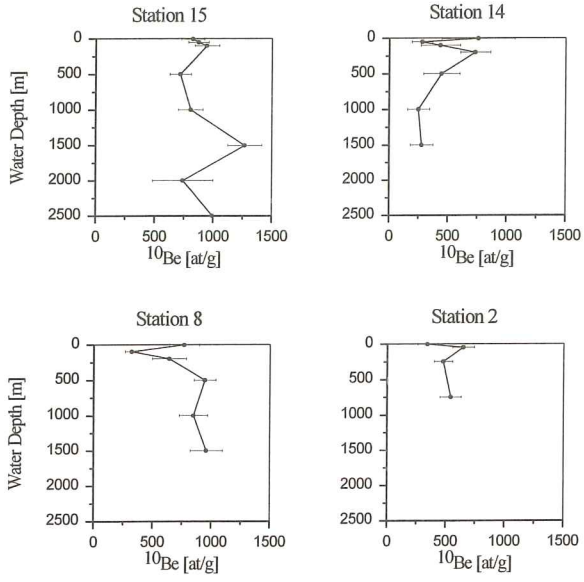


Figure 7: $^{10}$Be concentrations versus water depth [m].

*$^{10}$Be in the Arctic water column and in the Laptev Sea*

We measured $^{10}$Be profiles at 4 stations in the Norwegian- and in the Greenland Sea. The localities of the water profiles are listed in Table 2 and shown in Figure 7. The deep water concentrations of $^{10}$Be at stations 8 and 15 (Norwegian current) come close to the value of Atlantic deep water (ranging between 1000 and 1500 at/g, Segl et al., 1987), whereas stations 2 and 14 (East Greenland Current) show deep water concentrations lower than the NADW. The deep water concentration at station 14 probably reflects Arctic deep water conditions. Three further profiles of $^{10}$Be from the central Arctic Ocean sampled during the campaign ARK VIII/3 are plotted in Figure 8. They show nearly constant $^{10}$Be concentration around 500 at/g. The values are lower than the concentrations in the Atlantic deep water and at least one order of magnitude lower than the concentrations near the mouth of the Lena of 5000 at/g. The high concentrations in the water masses of the Laptev Sea near the mouth of the river Lena (PM

9463-1 and PM 9472-3; Table 8) reflect the input of continental $^{10}Be$ with the rivers. Comparison with the profiles in the central Arctic Ocean clearly shows that the high concentration of $^{10}Be$ near the mouth of the Laptev Sea does not reach the central part of the Arctic Ocean. We therefore conclude that it is being scavenged close to its continental source. This conclusion corroborates the very high fluxes of $^{10}Be$ into shelf sediments derived above, suggesting that riverine $^{10}Be$ is adsorbed on aluminosilicates (Southon et al., 1987, Jansen et al., 1987) and rapidly sedimented.

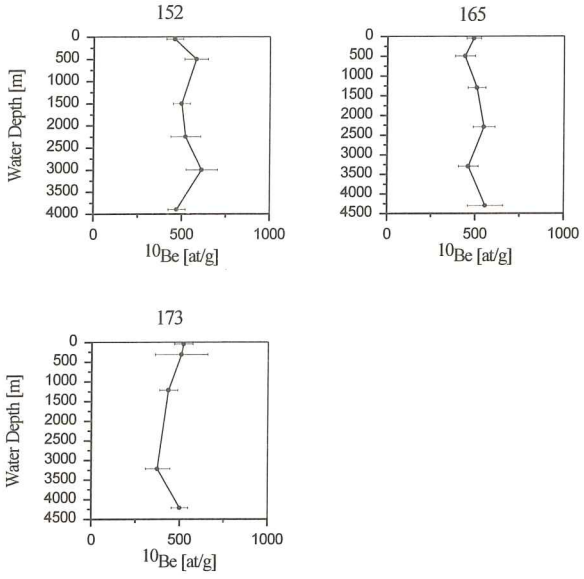


Figure 8: $^{10}Be$ concentrations versus water depth [m].

Table 8: $^{10}Be$ concentrations of water samples from the Laptev Sea.

| Station | Water Depth [m] | $^{10}Be$ [atoms/g] |
|---|---|---|
| PM 9463-1 | 2 | 2150 ± 300 |
| PM 9463-1 | 30 | 3135 ± 520 |
| PM 9472-3 | 2 | 5740 ± 600 |
| PM 9494-3 | 2 | 895 ± 200 |

*Sedimentary $^{10}Be$-Fluxes in the continental slope of the Laptev Sea*

To test if significant amounts of terrigenic $^{10}Be$ may still be transferred into the central Arctic Ocean, we measured the $^{10}Be$ concentrations and $^{230}Th_{ex}$ activities of the sediment core PS 2471-4 from the continental slope of the Laptev Sea. This core is located about 500 km from the mouth of the Lena. The average sedimentation rates for each oxygen isotope stage (Table 8) of this core were determined by biostratigraphy (Fahl, pers. comm.) and from the depth profile

of the $^{230}Th_{ex}$ activity. As presented by Nürnberg et al. (1995) the upper 50 cm of this sediment core can be associated with the oxygen isotope stage 1. Further the abundance of Gephyrocapsa spp. in the core section between 200 and 300 cm was related to the isotope oxygen stage 5. However Baumann (1990) showed that in sediments from the Nansen Basin, the coccolithophoride Gephyrocapsa spp. was also recorded in the oxygen isotope stage 3. $^{230}Th_{ex}$, $^{10}Be$, microfossils and amino acids deliver further stratigraphic information.

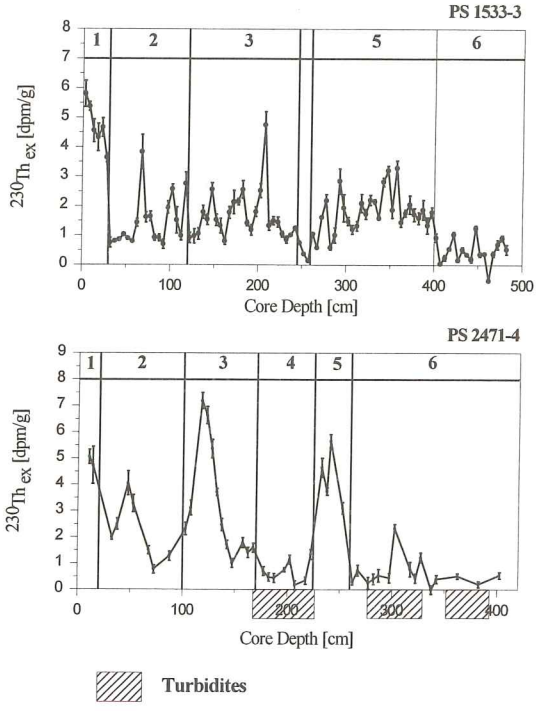


Figure 9: $^{230}Th_{ex}$ activities of the sediment cores PS 1533-3 and PS 2471-4 versus core depth [cm].

## $^{230}Th_{ex}$ and $^{10}Be$

In this study we compare the $^{230}Th_{ex}$- and $^{10}Be$ profiles of PS 2471-4 (Figure 9, Figure 10) with the radionuclide profiles of PS 1533-3 from the Yermak Plateau (Eisenhauer et al., 1994), where an age-depth model is available. Characteristic for the $^{230}Th_{ex}$ profile of core PS 1533-3 and of other sediment cores from high northern latitudes are two dominant features in the $^{230}Th_{ex}$ profiles. These are marked by a rather abrupt drop of the $^{230}Th_{ex}$ activity at the stage boundaries 6/5 and 2/1 (Scholten et al., 1994). By analogy we related the stage boundary 6/5 of PS 2471-4 at a core depth of 265 cm. Because of missing $^{230}Th_{ex}$ data for the upper 15 cm of the core, the transition at 2/1, fixed at a depth of 20 cm, is rather uncertain. According to this model the three turbitide layers were deposited during the glacial stages 4 and 6. The comparison of the $^{10}Be$-profile to that of core PS 1533-3 confirms the age-depth model derived from $^{230}Th_{ex}$. From the $^{10}Be$ concentrations we calculated the depositional $^{10}Be$ fluxes during the isotopic stages 2, 3 and 5 (Table 9). The average $^{10}Be$ flux amounts to [$(2.32 \pm 0.50) \cdot 10^6$ at $cm^{-2}$ $a^{-1}$]. It is by at least one order of magnitude lower than the flux in the shelf area, but higher than the fluxes of [$(0.1 - 0.6) \cdot 10^6$ at $cm^{-2}$ $a^{-1}$] in the central part of the Arctic Ocean (Strobl et al., in prep.). We did not evaluate the flux during stage 4 because the sedimentation

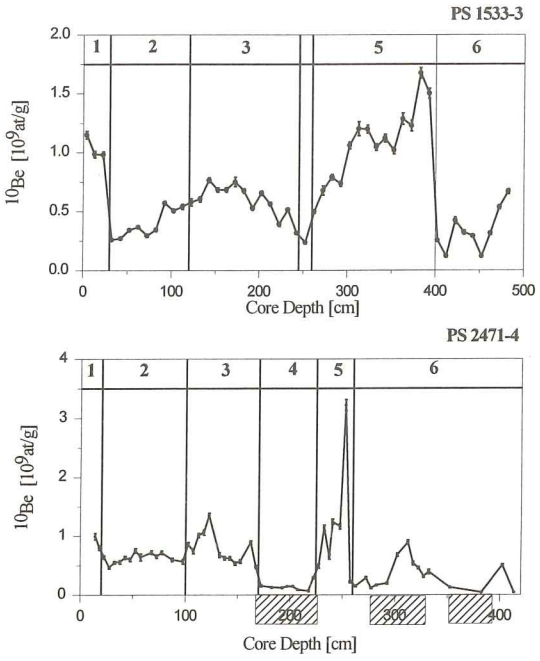


Figure 10: $^{10}$Be concentrations of the sediment cores PS 1533-3 and PS 2471-4 versus core depth [cm].

Table 9: Sedimentation rates and the depositional $^{10}$Be fluxes during the isotope stages 2, 3 and 5 of the sediment core PS 2471-4.

| Oxygen Isotope Stage | Sedimentation rate [cm ka$^{-1}$] | Depositional $^{10}$Be Flux [$10^6$ atoms cm$^{-2}$ a$^{-1}$] |
|---|---|---|
| 2 | 5.80 ± 0.80 | 4.10 ± 0.50 |
| 3 | 1.86 ± 0.30 | 1.96 ± 0.30 |
| 5 | 0.54 ± 0.20 | 0.90 ± 0.10 |

rate during this oxygen isotope stage is highly uncertain. As the fluxes of $^{230}Th_{ex}$ are close to the expected production flux, we can exclude that the $^{10}$Be fluxes were distorted by processes of sediment redistribution or enhanced scavenging. The depositional $^{10}$Be-fluxes of the cores PM 9482-1, PM 9463-8, PM 9462-1 and PS 2471-4 (oxygen isotope stage 3) are presented im Figure 11. The conclusion from the rather low $^{10}$Be flux on the continental slope is that only a smaller part of the terrigenic $^{10}$Be finds its way to the Arctic Ocean.

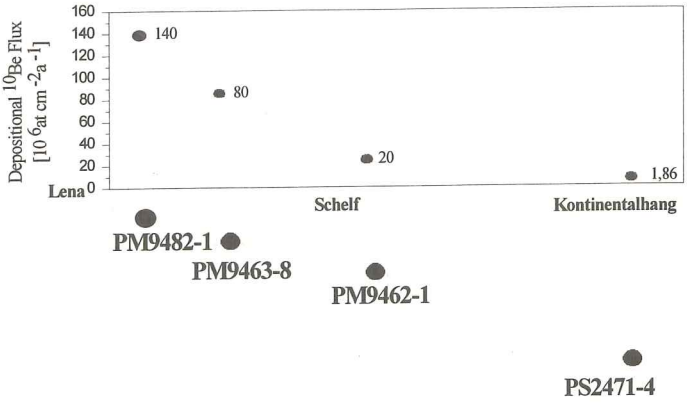


Figure 11: Depositional $^{10}Be$ fluxes in the shelf area of the Laptev Sea and on the continental slope.

## Conclusions

We conclude that the rivers are the main source of $^{10}Be$ in the shelf areas of the Arctic Ocean. From the comparison of the fluxes of $^{10}Be$ in the central Arctic Ocean, on the continental slope and in the shelf area of the Laptev Sea we further conclude that most of the $^{10}Be$ delivered to the shelf area by the rivers Lena, Yana and Kathanga must be deposited directly in the shelf area.

## Acknowledgments

The financial support by the German Ministry of Education, Science, Research and Technology (BMBF) is gratefully acknowledged. The authors want to thank M. v. de Loeff, J. Scholten, T. Eisenhauer and T. Billen for sampling and the availabiltity of water samples from the central Arctic Ocean, the Norwegian- and Greenland Sea. The chemical preparation and measurement of the water samples from the Norwegian- and Greenland Sea were done by H.J. Rutsch and M. Frank.

## References

Arnold, T. (1989) Bestimmung von Mischungskoeffizienten in der Norwegischen See mit $^{210}Pb$. Diplomarbeit Universität Heidelberg.

Baumann, M. (1990) Coccoliths in sediments of the eastern Arctic Basin. In: Geological History of the Polar Ocean: Arctic versus Antarctic, NATO Series C, Mathematical and Physical Sciences, Bleil, U. and J. Thiede (eds), 308, 437-445.

Benninger, L.K, R.C. Aller, J.K. Cochran, and K.K. Turekian (1979) Effects of biological sediment mixing on the $^{210}Pb$ chronology and trace metal distribution in a Long Island Sound sediment core. Earth Planet. Sci. Lett., 43, 241-259.

Berner, R.A. (1980) Early diagenesis - a theoretical approach. Princeton University Press, Princeton.

Bollhoefer, A., A. Mangini, A. Lenhard, M. Wessels, F. Giovanoli and B. Schwarz (1994) High-Resolution $^{210}Pb$-Dating of Lake Constance Sediments; Stable Lead in Lake Constance. Environ. Geol., 24, 267-274.

Doerr, H. and K.O. Muennich (1991) Lead and Cesium Transport in European Forest Soils. Water Air and Soil Pollution, 57-58, 808-818.

Dominik, J., A. Mangini and G. Mueller (1981) Determination of recent deposition rates in Lake Constance with radioisotopic methods. Sedimentology, V28, 653-677.

Eisenhauer, A., R.F. Spielhagen, M. Frank, G. Hentzschel, A. Mangini, P.W. Kubik, B. Dittrich-Hannen and T. Billen, $^{10}$Be records of sediment cores from high northern latitudes, Earth and Planet. Sci. Lett., 124, 171-184, 1994.

Evans, D.W., J.J. Alberts and A.C. Clark (1983) Reversible ion-exchange fixation of cesium-137 leading to mobilization from reservoir sediments. Geochimica et Cosmochimica Acta, Vol. 47, 1041-1049.

Finkel, R., S. Krishnaswami and D.L. Clark (1977) $^{10}$Be in Arctic ocean sediments. Earth and Planet. Sci. Lett,. 35, 199-204.

Frank, M. (1996) Reconstruction of Late Quaternary environmental conditions applying the natural radionuclides $^{230}$Th, $^{10}$Be, $^{231}$Pa and $^{238}$U: A study of deep-sea sediments from the eastern sector of the Antarctic Current System. Ber. Polarforschung, 186, 136 pp.

Fütterer, D.K. (1992) Arctic'91: Die Expedition ARK-VIII/3 mit FS Polarstern. Reports on Polar Research, 107, 142pp.

Fütterer, D.K. (1994) Die Expedition Arctic'93. Der Fahrtabschnitt ARK-IX/4 mit FS Polarstern. Reports on Polar Research, 149, 244 pp.

Gopalakrishnan, S., C. Rangarajan, L.U. Joshi, D.K. Kapoor and C.D. Eapen (1973) Measurements on airborne and surface fallout radioactivity in India. Government of India, Atomic Energy Commission, Bhabha Atomic Research Centre, Bombay, India.

Graustein, W.C. and K.K. Turekian (1989) The effects of forests and topography on the deposition of sub-micrometer aerosols measured by lead-210 and cesium-137 in soils. Agricultural and Forest Meteorology, 47, 199-220.

Henken-Mellies, W.-U., J. Beer, F. Heller, K.-J. Hsü, C. Shen, G. Bonani, H.-J. Hofmann, M. Suter and W. Wölfli (1990) $^{10}$Be and $^{9}$Be in South Atlantic DSDP site 519: Relation to geomagnetic reversals and to sediment composition. Earth Planet. Sci. Lett., 98, 267-276.

Jansen, J.H.F., C. Alderliesten, A.J. van Bennekom, K. van der Borg and A.F.M. de Jong (1987) Terrigenous supply of $^{10}$Be and dating with $^{14}$C and $^{10}$Be in sediments of the Angola Basin (SE Atlantic), Nucl. Instr. Meth. Vol., B29, 311-316.

Kassens, H. (1995) Laptev Sea System: Expeditions in 1994. Reports on Polar Research, 182, 195pp.

Langner, C. and Transdrift I Shipboard Party (1995) Distribution of Fe and Mn in pore waters and sediments of the Laptev Sea-Results of the expedition Transdrift I. In: Russian-German Cooperation: Laptev Sea System, Reports on Polar Research, 176, H. Kassens, D. Piepenburg, J. Thiede, L. Timokhov, H.-W. Hubberten, and S.M. Priamikov (eds), 387pp.

Lao, Y., R.F. Anderson, W.S. Broecker, S.E. Trumbore, H.J. Hofmann and W.Wölfli (1992a) Increased production of cosmogenic $^{10}$Be during the last glacial maximum. Nature, 357, 576-578.

Lao, Y., R.F. Anderson, W.S. Broecker, S.E. Trumbore, H.-J. Hofmann and W. Wölfli (1992b) Transport and burial rates of $^{10}$Be and $^{231}$Pa in the Pacific Ocean during the Holocene period. Earth and Planet. Sci. Lett., 113, 173-189.

Mangini, A., M. Segl, G. Bonani, H.-J. Hofmann, E. Morenzoni, M. Nessi, M. Suter, W. Wölfli and K.K. Turekian (1984) Mass spectrometric Beryllium dating of deep-sea sediments applying the Zürich tandem accelerator. Nucl. Instrum. Methods Phys. Res., B5, 353-357.

Mangini, A., M. Segl, H. Kudrass, M. Wiedicke, G. Bonani, H.-J. Hofmann, E. Morenzoni, M. Nessi, M. Suter, and W. Wölfli (1986) Diffusion and supply rates of $^{10}$Be and $^{230}$Th radioisotopes in two manganese encrustation from the South China Sea. Geochim. et Cosmochim. Acta 50, 149-156.

Monaghan, M.C., S. Krishnaswami and K.K Turekian (1985/1986) The global-average production rate of $^{10}$Be. Earth and Planet. Sci. Lett., 76, 279-287.

Nürnberg, D., D. Fütterer, F. Niessen, N. Nörgaard-Petersen, C. Schubert, R.F. Spielhagen and M. Wahsner (1995) The depositional environment of the Laptev Sea continental margin: Preliminary results from the RV „Polarstern„ ARK-IX/4 cruise. Polar Research, 14, 43-53.

Rehfeld, S. (1994) Deposition radioaktiver Tracer in einem Transportmodell der Atmosphäre. Thesis, Univ. Hamburg, 144pp.

Robbins, J.A. and D.N. Edgington (1976) Depositional processes and the determination of recent sedimentation rates in Lake Michigan. Proc. 2nd Federal Conf. Great Lakes, 378-390.

Scholten, J.C., R. Botz, H. Paetsch and P. Stoffers (1994) $^{230}Th_{ex}$ flux into Norwegian-Greenland sediments: Evidence for lateral sediment transport during the past 300,000 years. Earth and Planet. Sci. Lett., 121, 111-124.

Segl, M, A. Mangini, J. Beer, G. Bonani, M. Suter and W. Wölfli (1987) $^{10}$Be in the Atlantic Ocean, a transect at 25°N. Nucl. Instr. Meth., B29, 332-334.

Southon , J.R., T.L. Ku, D.E. Nelson, J.L. Reyss, J.S. Vogel (1987) $^{10}$Be in a deep sea core: implications regarding $^{10}$Be production changes over the past 420 ka. Earth Planet. Sci. Lett., 85, 356-364.

Stanzick, A. (1996) Räumliche und zeitliche Depositionsvariationen der Radioisotope $^{10}$Be und $^{210}$Pb in Eisbohrkernen Zentralgrönlands. Diploma thesis, Institut für Umweltphysik Heidelberg, Germany, 96pp.

Thiede, J. and G. Hempel (1991) Die Expedition Arktis-VII/1 mit FS Polarstern. Reports on Polar Research, 80, 137pp.

Turekian, K.K., Y. Nozaki and L.K. Benninger (1977) Geochemistry of atmospheric radon and radon products. Ann. Rev. Earth Planet. Sci., 5, 227-255.

von Gunten, H.R. and R.N. Moser (1993) How reliable is the $^{210}$Pb dating method? Old and new results from Switzerland. Journal of Paleolimnology, 0, 1-18.